

Synthesizing Diverse Human Motions in 3D Indoor Scenes

Kaifeng Zhao¹, Yan Zhang¹, Shaofei Wang¹, Thabo Beeler², and Siyu Tang¹

¹ETH Zürich

²Google



Figure 1: Interaction with environments is one core ability of virtual humans and remains a challenging problem. We propose a method capable of generating a sequence of natural interaction events in real cluttered scenes as illustrated in this figure. The human first walks to sit on a stool (yellow to red), then walk to another chair to sit down (red to magenta), and finally walk to and lie on the sofa (magenta to blue).

Abstract

We present a novel method for populating 3D indoor scenes with virtual humans that can navigate the environment and interact with objects in a realistic manner. Existing approaches rely on high-quality training sequences that capture a diverse range of human motions in 3D scenes. However, such motion data is costly, difficult to obtain and can never cover the full range of plausible human-scene interactions in complex indoor environments. To address these challenges, we propose a reinforcement learning-based approach to learn policy networks that predict latent variables of a powerful generative motion model that is trained on a large-scale motion capture dataset (AMASS). For navigating in a 3D environment, we propose a scene-aware policy training scheme with a novel collision avoidance reward function. Combined with the powerful generative motion model, we can synthesize highly diverse hu-

man motions navigating 3D indoor scenes, meanwhile effectively avoiding obstacles. For detailed human-object interactions, we carefully curate interaction-aware reward functions by leveraging a marker-based body representation and the signed distance field (SDF) representation of the 3D scene. With a number of important training design schemes, our method can synthesize realistic and diverse human-object interactions (e.g., sitting on a chair and then getting up) even for out-of-distribution test scenarios with different object shapes, orientations, starting body positions, and poses. Experimental results demonstrate that our approach outperforms state-of-the-art human-scene interaction synthesis frameworks in terms of both motion naturalness and diversity. Video results are available on the project page: <https://zkf1997.github.io/DIMOS>.

1. Introduction

Simulating how humans behave in and interact with environments plays an essential role in many applications, such as generating training data for machine learning algorithms, simulating autonomous agents in interactive applications such as AR/VR or computer games, informing architectural designs, optimizing environments for assembly-line work, and many more. Although this task is highly related to character animation in graphics, most existing character animation methods (e.g. [13, 3, 2]) focus on improving the realism and controllability of character movement. With these traditional character animation workflows, one can simulate body movements but can not generate natural human behaviors, since the characters are not autonomous, and cannot spontaneously interact with the surroundings in diverse plausible ways as real humans. This results in inferior naturalness and stochasticity and limits the utility for example for architecture design, smart shopping, autonomous driving, and other appealing applications.

To overcome such limitations, our goal is to breathe life into digital humans, so that they can behave spontaneously and move autonomously in environments based on cognitive goals. To achieve this, we leverage reinforcement learning (RL) [40] to formulate our task. By designing goals as rewards, perceptions as states, and neural latent variables as actions, we can synthesize continuous, stochastic, physically plausible, and spontaneous behavior of virtual humans to inhabit the digital world.

Although existing RL-based motion synthesis approaches (e.g. [21, 53, 28]) can effectively generate natural behavior to achieve goals, their generated virtual humans can only interact with simple scenes, rather than complex environments with functional furniture and objects. For example, GAMMA [53] employs generative motion primitives and a policy network that are generalizable across diverse human bodies, but it can only synthesize waypoint-reaching behavior with unbounded locomotions. The trained digital humans are not aware of how to perform actions like sitting on a chair or lying on a sofa, and frequently inter-penetrate with the scene geometry.

To overcome these limitations, we propose two methods to make virtual humans scene-aware. First, in order to achieve controllable high-level interactions, we provide fine-grained guidances based on body surface markers [51] generated from COINS [54]. Specifically, we use COINS [54] to generate human bodies interacting with scene objects given the interaction semantics, and then use the body markers as the interaction guidance for motion synthesis. With the help of reinforcement learning, the virtual human can autonomously reach the target location and mimic the target pose in a variety of plausible ways. Second, we design new policies to help virtual humans avoid collisions with scene objects, in order to achieve physically

plausible low-level human-scene interaction. Specifically, we use navigating mesh to generate a set of waypoints in a cluttered scene [8, 35], then we use a local collision-aware state to incorporate scene information into the locomotion policy. We train the policy network in synthetic scenes consisting of random obstacles to learn generalizable scene-aware locomotion. For close object interaction, we add features derived from the signed distance of body markers to the object surface and the distance gradient direction to encode the proximity between humans and objects. Therefore, by specifying ‘sitting on the sofa’, our approach will drive virtual humans to autonomously move to the target place and sit in various natural ways, as how a real human behaves.

With this framework, we investigate how to synthesize behavior with unbounded motions consisting of locomotion, sitting, and lying. We empirically evaluate the motion realism and interaction performance of our proposed human-scene interaction synthesis method through experiments. Our results demonstrate that the generated motion sequences have consistently better quality compared to the baselines, in terms of the diversity, physical plausibility, and perceptual scores.

In summary, we aim to let virtual humans inhabit virtual environments, and present these contributions:

1. We propose a reinforcement learning-based framework to generate realistic and diverse behaviors of virtual humans in complex indoor scenes.
2. We leverage COINS [54] to generate the detailed interaction goal from interaction semantics and use body surface markers as the guidance for motion synthesis, in order to make the virtual humans controllable via interaction semantics and fine-grained body poses.
3. We design scene and interaction-aware policies to enable virtual humans to navigate 3D scenes while avoiding collisions, to interact with scene objects, and to continuously perform sequences of activities in complex scenes.

Code and models will be publicly released.

2. Related Work

Human motion synthesis. Generating high-quality human motion has been widely explored in computer vision and graphics. Motion graph [18] and motion matching [2, 3, 56] generate motion by searching suitable clips in datasets and blending them automatically. Starke *et al.* [37, 38, 36] use phase-conditioned neural networks to synthesize character animations and interaction with objects. Zhang *et al.* [51, 53] model motion as sequences of surface markers on the parametric SMPL-X [26] body model,

and train autoregressive networks on the large-scale mocap dataset AMASS [24] in order to produce diverse motions of bodies with various shapes. Peng *et al.* [28] use imitation learning with a skill discovery objective to learn a general motion skill space for physically simulated characters. Tang *et al.* [41] trains a motion manifold model of consecutive frames for real-time motion transition. Li *et al.* [19] propose a generative adversarial network to synthesize motions from one single motion sequence. Transformer-based models have been designed to predict or generate stochastic motions conditioned on action categories [30], texts [31, 42], gaze [55], and others. More recently, diffusion model-based motion methods [43, 48, 44] achieve appealing performance on motion synthesis conditioned on various control signals and demonstrate flexible motion editing.

Motion control and RL-based behavior synthesis. Various motion control methods have been proposed to constrain body movements or guide the body to reach goals. Sampling-based motion control methods [23, 22] generate multiple samples at each step and select the samples that best match the targets. Goal-conditional generation networks [7, 17, 14] are applied for motion control. However, such methods may produce invalid results when the training domain gap is large. Optimization-based motion control methods [15, 47] leverage the learned generative motion model as regularization and optimize the motion latent variables to fit the decoded motion to the goals. Motion diffusion models [43, 48] implement control via classifier-free text guidance or gradually reprojecting the generated motion onto the physically plausible space at individual denoising steps. Human motions can be formulated as a Markov decision process, and synthesized and controlled via RL. Imitation learning methods [27, 1, 29, 25] trains policy networks to control humanoids to imitate reference motion and complete given tasks. Peng *et al.* [28] propose a skill discovery objective apart from the imitation objective to learn a latent space for general motion skills and train substream task policies leveraging the general motion space. Ling *et al.* [21] and Zhang *et al.* [53] leverage the latent variable of the generative motion model as the action, and train policies to generate high-fidelity perpetual motions.

Human-scene interaction synthesis. Synthesizing natural human-scene interactions is an appealing direction in recent years. Object affordance [5, 33, 16, 6] provides cues about how humans can interact with scene objects. Static bodies interacting with scene objects can be generated based on the scene semantics, geometries, and interaction semantics [20, 11, 49, 52, 54]. Wang *et al.* [46] propose to train generative models for human motion in scenes conditioned on scene pointclouds. Wang *et al.* [45] propose a three-stage method to synthesize human motions in

scenes, which first puts static bodies in scenes, then generates global paths, and afterwards synthesizes in-between motions. Starke [37] propose an autoregressive neural state machine to synthesize character animations interacting with objects. Hassan *et al.* [9] and Zhang *et al.* [50] propose similar networks as in [37], and incorporate stochastic motion generation and finer-grained motion control modules. Peng *et al.* [28] trains policy to control physically-simulated characters to hit a box. Hassan *et al.* [12] extend the method to generate interactions like carrying a box or sitting on a chair.

Ours versus others. Our method is most similar to GAMMA [53] and SAMP [9]. GAMMA learns generalizable motion models and policies across human bodies of diverse identities and shapes, without goal-motion paired data. Despite producing high-fidelity motions, its results are restricted to locomotion in the scene, and frequently collide with the scene objects. SAMP learns conditional VAEs to produce inhabiting actions in living environments, with object-motion paired data. Its generated motion has visible artifacts like foot-ground skating. Our method combines their merits and discards their individual disadvantages. We significantly extend the RL-based framework proposed in GAMMA by incorporating fine-grained motion controls (generated by interaction semantics) and scene interaction modules, so as to generate inhabiting actions in complex daily living environments. Compared to SAMP, our produced motion is more diverse, more physically plausible, and can be guided by fine-grained body surface markers. For systematical comparisons, please refer to Section 4.

3. Method

3.1. Preliminaries

SMPL-X [26] and body representation. We use SMPL-X to represent the bodies in our work. Given the shape parameter $\beta \in \mathbb{R}^{10}$ and the body pose parameter $\theta \in \mathbb{R}^{63}$, SMPL-X produces a posed body mesh with a fixed topology of 10475 vertices. To place the body in the scene, the root location $\mathbf{r} \in \mathbb{R}^3$ and the orientation $\phi \in \mathfrak{so}(3)$ w.r.t. the world coordinates are additionally needed. Since facial expressions and hand gestures are not our focus, we leave their parameters as the default values. In addition, we follow [51, 53] to represent the body in motion by the *SSM-67* body surface marker placement, which effectively represents the body degrees-of-freedom (DOFs) within the Euclidean space. A motion sequence is then formulated as $\mathbf{X} = \{\mathbf{x}_1, \dots, \mathbf{x}_N\}$, where N is the length of motion and $\mathbf{x}_i \in \mathbb{R}^{67 \times 3}$ denotes the body marker 3D locations at frame i . The marker locations are relative to a canonical coordinate frame centered at the first frame body pelvis.

GAMMA [53]. GAMMA can synthesize stochastic, perpetual, and realistic goal-reaching actions in 3D scenes. It comprises generative motion primitive models, RL-based control, and tree-based search to implement gradient-free test-time optimization. The motion primitive is formulated by a CVAE model to generate uncertain marker motions for 0.25 seconds into the future given a motion seed, followed by a MLP-based body regressor to yield SMPL-X parameters. Long-term random motion can be generated by running the motion primitive model recursively. The RL-based control is implemented by learning a policy within a simulation area. The actor-critic framework [40] and the PPO algorithm [34] are applied to update the policy network. An additional motion prior term is used to ensure the motion appears natural. During testing, the generated motion primitives are stored in a tree structure. The best K primitives are preserved and used as the new motion seeds, and the rest is discarded. Since the motion primitive models and the policy are learned on diverse human bodies, GAMMA is generalizable across virtual humans with various body shapes and identities.

COINS[54]. COINS generates physically plausible static human-scene interactions with instance-level semantic control. Given the point cloud of the object and action labels, COINS can generate static bodies interacting with the given object using the specified action, *e.g.*, sitting, lying, or touching. COINS leverages transformer-based generative models trained on a human-scene interaction dataset [10] to first generate a plausible body pelvis for interaction and then the posed body. The generated bodies are further optimized to improve the physical plausibility and to match the predicted action-dependent contact areas with objects. Such generated static bodies capture the characteristics of the human-scene interaction process and can be used as fine-grained interaction guidance.

3.2. RL-based Framework to Inhabit the Virtual

As illustrated in Fig. 2, we propose a behavior synthesis framework that enables virtual humans to navigate complex indoor scenes and interact with various scene objects, *e.g.*, sitting on a chair. Compared to the GAMMA framework [53], our method incorporates scene information into the states to better handle the complex human-scene interactions. Also, we use body marker goals to provide fine-grained guidance on how to pose the body at the target location. With modularized path-finding methods and static person-scene interaction generation methods, our framework can synthesize realistic inhabiting behavior. In our work, we use COINS [54] for static person-scene interaction generation because of its superior performance and controllability via ‘verb-noun’ language phrases. The walking path can be either generated by hand, or by automatic

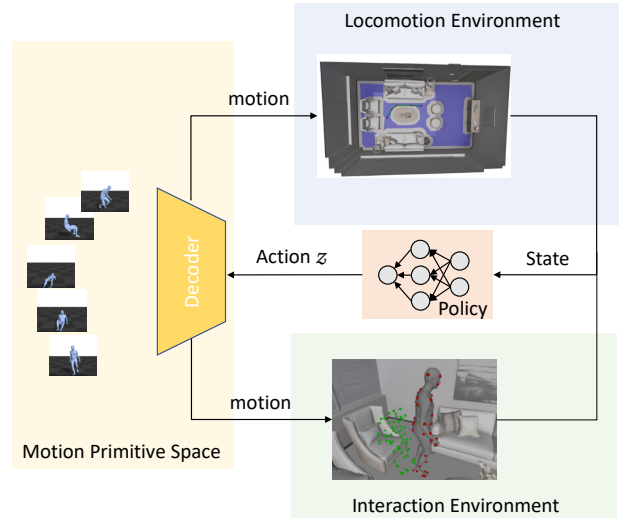


Figure 2: Illustration of our proposed human-scene interaction synthesis framework, which consists of motion model learning, policy learning, and tree-based search for test-time optimization. Combining off-the-shelf path finding methods and static person-scene interaction generation methods, we can synthesize realistic inhabiting behavior of virtual humans with fine-grained control.

path-finding algorithms like A* [35, 8].

We formulate behavior synthesis with reinforcement learning. At each time step, the virtual human perceives its state s_t in the environment and samples an action a_t from its policy model $\pi(a_t|s_t)$. Based on its motion model, it advances its motion state, and obtains a new perception state s_{t+1} . A reward $r_t = r(s_t, a_t, s_{t+1})$ is calculated, tailored to different behaviors.

The motion model and the action. We leverage the CVAE-based generative motion primitive [53] as our motion model, and use its latent variable as the action. We train the model conditioned on 1 or 2 past frames using the combination of the SAMP [9] and AMASS [24] motion capture datasets, so as to learn a latent motion primitive space covering motion skills for human-scene interactions. Each latent variable z in the motion primitive space is regarded as an action and can be decoded to a short clip of motion.

The state. The state is formulated by

$$s_t = (X_s, I, G), \quad (1)$$

where $X_s \in \mathbb{R}^{M \times 67 \times 3}$ is the body markers motion seed that represents a motion history of M frames. I and G denote the person-scene interaction feature and the goal-reaching feature, respectively. The interaction feature and

goal-reaching feature vary among the locomotion and object interaction tasks. We introduce the detailed formulation in Sec. 3.3 and 3.4.

The rewards. The rewards evaluate how well the virtual human performs locomotion and fine-grained interaction tasks. We formulate rewards as

$$r = r_{goal} + r_{contact} + r_{pene}, \quad (2)$$

where r_{goal} , $r_{contact}$ and r_{pene} represent the rewards for goal-reaching, foot-ground contact, and collision avoidance, respectively. Specifically, the contact reward $r_{contact}$ encourages foot-floor contact and discourages foot skating, and is defined as:

$$r_{contact} = e^{-(|\min_{x \in F} x_z| - 0.05)_+} \cdot e^{-(\min_{x \in F} \|x_{vel}\|_2 - 0.075)_+}, \quad (3)$$

where F is the set of foot markers, x_z is the height of the markers, x_{vel} is the velocity of the markers, and $(\cdot)_+$ denotes clipping negative values. There are tolerance thresholds of 0.05m for foot-floor distance and 0.075m/s for skating, following GAMMA [53]. The other two reward terms are action-specific and introduced in Sec. 3.3 and 3.4.

Policy network and training. We use the actor-critic algorithm [40] to learn the policy, where a policy network and a value network are trained jointly. The policy network generates a diagonal Gaussian distribution representing the stochastic action distribution given a state, while the value network outputs the value estimation for each state.

Like in GAMMA [53], these two networks are jointly trained by minimizing:

$$\mathcal{L} = \mathcal{L}_{PPO} + \mathbb{E}[(r_t - V(s_t))^2] + \alpha \text{KL-div}(\pi(z|s) || \mathcal{N}(0, I)), \quad (4)$$

where the first term is the PPO [34] loss, the second updates the value estimation of the critic networks, and the third Kullback–Leibler divergence term regularizes motion in the latent space [53].

In the following, we elaborate how the states and rewards are designed for different actions, i.e. locomotion and fine-grained scene object interaction. Therefore, long-term and coherent behavior can be composed by rolling out the initial body configuration and switching between the locomotion and object interaction stages.

3.3. Scene-Aware Locomotion Synthesis

Navigating in cluttered scenes expects the human body to move to the target, while avoiding collisions with scene objects.

Our key idea is to incorporate the walkability information of the surrounding environment into the states and use

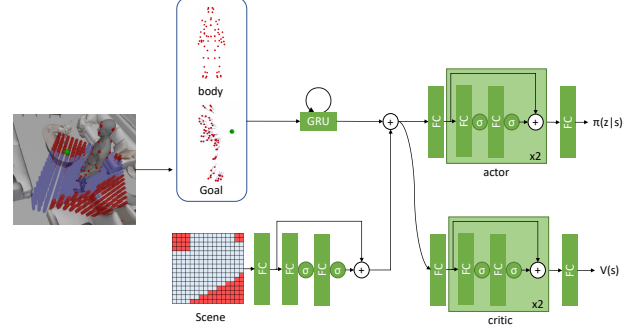


Figure 3: Illustration of the scene-aware locomotion policy network. The locomotion policy state consists of the body markers, the goal-reaching feature of normalized direction vectors from markers to the goal pelvis, and the interaction feature of a 2D binary map indicating the walkability (red: non-walkable area, blue: walkable area) of the local $1.6m \times 1.6m$ square area. The locomotion policy network employs the actor-critic architecture and shares the state encoder.

collision rewards to train the locomotion policy in order to avoid scene collisions. Specifically, we represent the walkability of the environment surrounding the human agent using a 2D binary map $\mathcal{M} \in \{0, 1\}^{16 \times 16}$ as illustrated in Fig. 3.

The walkability map is defined in the human’s local coordinates and covers a $1.6m \times 1.6m$ area centered at the body pelvis. It consists of a 16×16 cell grid where each cell stores a binary value indicating whether this cell is walkable or not. This local walkability map enables the policy to sense surrounding obstacles.

Referring to Eq. 1, the person-scene interaction feature is specified by

$$I = \text{vec}(\mathcal{M}), \quad (5)$$

in which $\text{vec}(\cdot)$ denotes vectorization. The goal-reaching feature is specified by

$$G = (\tilde{g}_p - X_s)_n, \quad (6)$$

where $X_s, \tilde{g}_p \in \mathbb{R}^{M \times 67 \times 3}$ are the body marker seed representing M frames history of body motion, and the broadcasted target pelvis location relative to the body-centered canonical coordinate, respectively. $(\tilde{g}_p - X_s)_n$ denotes the normalized vectors pointing from each marker to the goal pelvis.

The rewards contributing to Eq. 2 are defined as

$$r_{pene} = e^{-|\mathcal{M}_0 \cap \mathcal{B}_{xy}(X)|}, \quad (7)$$

where \mathcal{M}_0 denotes the non-walkable cells in the walkability map, $\mathcal{B}_{xy}(\cdot)$ denotes the 2D bounding box of the body markers X , \cap denotes their intersection, and $|\cdot|$ denotes the number of non-walkable cells within the bounding box of humans.

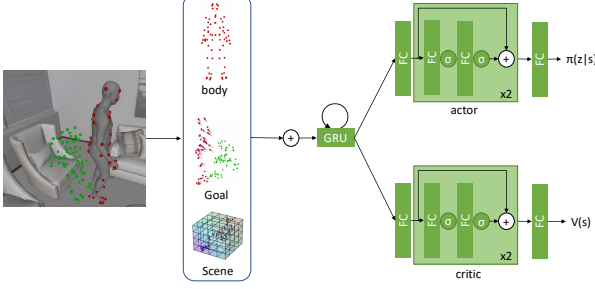


Figure 4: Illustration of the object interaction policy network. The interaction policy state consists of the body markers, the goal-reaching features of both distance and direction from current markers to the goal markers, and the interaction features of the signed distances from each marker to the object surfaces and the signed distance gradient at each marker location. Such interaction features encode the proximity relationship between the human and the interaction object.

$$r_{goal} = r_{dist} + r_{ori}, \quad (8)$$

$$r_{dist} = 1 - (\|\mathbf{p} - \mathbf{g}_p\|_2 - 0.05)_+, \quad (9)$$

$$r_{ori} = \frac{\langle \mathbf{o}, \mathbf{g}_p - \mathbf{p} \rangle}{2}, \quad (10)$$

where r_{dist} encourages the body pelvis \mathbf{p} to be close to the pelvis goal \mathbf{g}_p and r_{ori} encourages the body facing direction \mathbf{o} to be aligned with the direction from the current body pelvis \mathbf{p} to the pelvis goal \mathbf{g}_p .

3.4. Fine-grained Interaction Synthesis

To synthesize fine-grained interactions, *e.g.* sitting on a chair or lying on a sofa, we use marker targets as goals, and model the contact between the body surface and the scene object in a compact way. The target marker sets are generated by a static person-scene interaction method such as [49, 11, 54]. We use COINS [54] due to its superior performance and controllability via ‘verb-noun’ language phrases.

In addition to the marker-based goal guidance, we incorporate the proximity relations between humans and objects into the states. Specifically, we use the signed distance from each marker to the surface of the scene object, as well as the distance gradient direction to represent the proximity relationship, as illustrated in Fig. 4. Both signed distance and gradient direction are calculated using the objects signed distance field (SDF) Ψ_O .

Referring to Eq. 1, the person-scene interaction feature is formulated as

$$I = [\Psi_O(\mathbf{X}_s), \nabla \Psi_O(\mathbf{X}_s)], \quad (11)$$

in which $\Psi_O \in \mathbb{R}^{M \times 67}$ and $\nabla \Psi_O \in \mathbb{R}^{M \times 201}$ denote the SDF values and gradients at each marker location in the M frames, respectively, and $[\cdot]$ denotes feature concatenation. The goal-reaching feature is formulated as

$$G = [(\tilde{\mathbf{g}}_m - \mathbf{X}_s)_n, \|\tilde{\mathbf{g}}_m - \mathbf{X}_s\|_2], \quad (12)$$

in which $\mathbf{X}_s \in \mathbb{R}^{M \times 67 \times 3}$ denotes the body markers seed, $\tilde{\mathbf{g}}_m \in \mathbb{R}^{M \times 67 \times 3}$ denotes the broadcasted goal body markers, $(\tilde{\mathbf{g}}_m - \mathbf{X}_s)_n$ denotes the normalized vector representing the direction from each marker to the corresponding target marker, $\|\tilde{\mathbf{g}}_m - \mathbf{X}_s\|_2$ denotes the distance from each marker to target marker.

The interaction policy is trained using the reward defined in Eq. 2 with the following interaction-specific goal reward and penetration reward:

$$r_{goal} = 1 - (\|\mathbf{x} - \mathbf{g}_m\|_2 - 0.05)_+, \quad (13)$$

$$r_{pene} = e^{-\frac{1}{|V|} \frac{1}{T} \sum_{t=1}^T \sum_{i=1}^{|V|} |(\Psi_O(\mathbf{v}_{ti}))_-|}, \quad (14)$$

with $|V|$ being the SMPL-X mesh vertices, T denotes the number of frames in each motion primitive (equals to 10 in our study). The distance reward encourages the final frame body markers \mathbf{x} to be close to the goal body markers \mathbf{g}_m . The penetration reward penalizes all the body vertices within a motion primitive that have negative SDF values. We use body vertices instead of joints because human-object contact happens on the body surface and can be better detected using vertices.

Moreover, we train the interaction policy with a mixture of ‘sit/lie down’ and ‘stand up’ tasks. This training scheme enables the human agent to also learn how to stand up and transit from object interaction back to locomotion, which fulfills the loop of synthesizing a sequence of interaction activities.

4. Experiment

Motion Datasets. We combine the large-scale motion capture dataset AMASS [24] with SAMP [9] motion data to train the motion primitive models. Each sequence is first subsampled to 40 FPS and then split into 10 frames and 100 frames clips. Each motion clip is canonicalized using the first frame body. Specifically, we select AMASS sequences annotated with ‘sit’ or ‘lie’ in BABEL [32] and all motion data of SAMP to train the motion primitive model. We observed that extending SAMP motion data with AMASS dataset is the key to making interaction policies work.

Policy Training Environments. To train the scene-aware locomotion policy, we randomly generate synthetic cluttered scenes consisting of random objects from Shapenet [4]. The training scenes are rectangle scenes with various

Table 1: Evaluation of the locomotion task. The up/down arrows denote the score is the higher/lower the better and the best results are in bold.

	time ↓	avg. dist ↓	contact ↑	loco pene ↑
SAMP	5.97	0.14	0.84	0.94
GAMMA	3.87	0.03	0.94	0.94
Ours	6.43	0.04	0.99	0.95

sizes and populated with random numbers of objects from Shapenet. Random initial and target location pairs are sampled in the walkable areas using navigation meshes to train the locomotion policy.

To train the interaction policy, we use furniture from ShapeNet and retarget bodies [37] interacting with similar objects from PROX [10] dataset to the furniture to get marker interaction goals. At test time, we use COINS [54] to generate the marker interaction goals. During interaction policy training, we first randomly sample the furniture and interaction goal. Then we sample the initial body with random poses and locations in front of the object to train the interaction policy.

4.1. Evaluation on Locomotion

We randomly generate test scenes for locomotion in the same way as the training scenes. The virtual human is instructed to move from the random start point to the random target point while avoiding penetration with scene objects.

Baselines and metrics. We compare our method with SAMP [9] and GAMMA [53] for locomotion. The SAMP results are recorded by running the released Unity demo. The start and termination are manually determined so the reported completion time may be slightly higher than the actual time due to human response time. The evaluation metrics for locomotion include: 1) time from start point to target point or reaching the time limit, measured in seconds. 2) the average distance from the final body to the targets, measured in meters. 3) foot contact score encouraging the lowest feet joints on the floor and discouraging foot skating as defined in Eq. 3. We use body joints instead of markers to calculate the contact score because the marker set annotation for the SAMP body is missing. 4) locomotion penetration score indicating the percentage of body vertices that are inside the walkable areas according to the navigation mesh.

Table 1 shows the empirical evaluation results. Our method achieves a higher contact score (0.99) than both GAMMA (0.94) and SAMP (0.84) which indicates better foot-floor contact and less foot skating. Moreover, our method achieves the highest penetration score which indicates our scene-aware policy can better avoid scene collisions. Fig. 5 shows examples of locomotion tasks where GAMMA collides into the scenes while our scene-

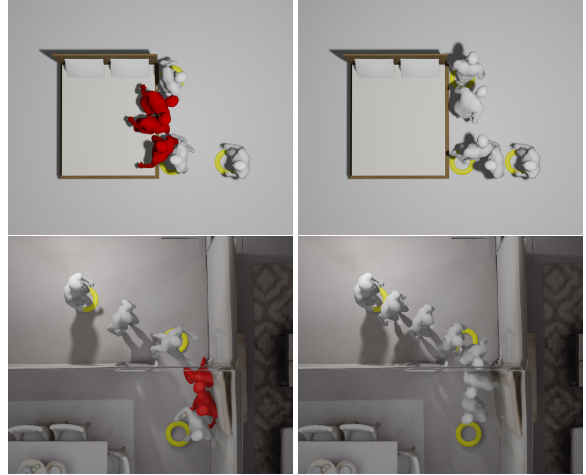


Figure 5: Demonstration of navigation tasks where GAMMA (left) collides with the obstacles (red bodies) while our scene-aware locomotion policy (right) avoids collision. The yellow circles denote the specified waypoints.

aware policy successfully avoids penetration. Compared to GAMMA trained in the same environments, we observe our scene-aware policy learns more conservative behavior with lower moving speed and spent more time (6.43s) walking to the target locations, just like a human afraid of stepping on surrounding traps. All the methods can reach the target location within a reasonable distance.

4.2. Evaluation on Interaction

We evaluate the object interaction task on 10 objects (3 armchairs, 3 straight chairs, 3 sofas, 1 L-sofa) from ShapeNet [4]. We use the real size annotation of the object models and manually filter to ensure the object sizes are reasonable for interaction. The virtual human is randomly placed in front of the target object and then instructed to perform the interaction, stay for around 2 seconds, and then stand up. We evaluate two interactions of sitting and lying separately.

Baselines and metrics. We compare our method with SAMP [9] for the object interaction task. The evaluation metrics for the interaction tasks are: 1) time of completing the object interaction task. 2) foot contact score as defined in Eq. 3. Note that the foot contact score does not always reflect the motion quality for lying tasks because the foot can often be off the floor during lying. 3) interaction penetration score for each frame is defined as:

$$s_{inter.pene} = \sum_{v_i \in V} |(\Psi_O(v_i))_-|, \quad (15)$$

Table 2: Evaluation of the interaction tasks. The up/down arrows denote the score is the higher/lower the better and the best results are in bold.

	time ↓	contact ↑	pene. mean ↓	pene. max ↓
SAMP sit	8.63	0.89	11.91	45.22
Ours sit	4.09	0.97	1.91	10.61
SAMP lie	12.55	0.73	44.77	238.81
Ours lie	4.20	0.78	9.90	44.61

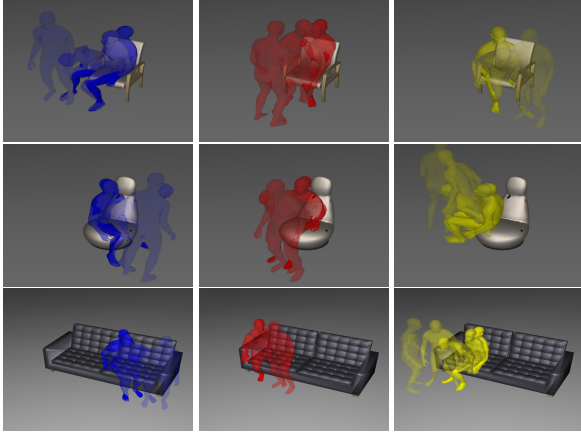


Figure 6: Demonstration of various object interactions with random initial body location and orientation. Each row shows generated interactions with one object and different colors denote different sequences generated by our method. Colors from transparent to solid denote time.

where Ψ_O is the object signed distance field, $(\cdot)_-$ clips all positive distance values to zero, and V is the body vertices. We show both the average penetration over time and the maximum penetration in one sequence.

Tab. 2 shows the evaluation results. Our method achieves a significantly higher foot contact score, indicating more natural motion. Our method also achieves lower mean and maximum penetration, which means our method generates more physically plausible results. Moreover, our method can complete the interaction tasks much faster than SAMP. This is because SAMP does not generalize well to unseen random body initialization and needs a longer time to start performing interactions.

Qualitative results demonstrating the various object interactions generated by our method are shown in Fig. 6. Our object interaction policy generalizes to random initial body locations and orientations.

4.3. Evaluation on Interaction in Cluttered scenes

Combining the scene-aware locomotion and object interaction modules, our method can generate a sequence of realistic human-scene interactions in cluttered environments.

Table 3: Evaluation of interaction in cluttered scenes. Here ‘contact’ denotes the foot contact score, ‘loco. pene.’ is the percentage of body vertices inside the walkable areas, ‘inter. pene. mean/max’ denotes the mean and maximum penetration with interaction objects, and ‘perceptual’ denotes the ratio of being chosen as perceptually more natural. The best results are in boldface.

	SAMP [9]	Ours
contact ↑	0.87	0.96
loco. pene. ↑	0.62	0.72
inter. pene. mean ↓	15.61	3.40
inter. pene. max ↓	101.25	39.68
perceptual. ↑	0.15	0.85

We conduct the empirical evaluation in real scene scan from Replica [39] and compare our method with SAMP. We select a list of interactable objects in the scene and instruct the virtual human to walk to the objects to perform interactions one by one. The evaluation metrics include the foot contact score, locomotion penetration score, and the mean and maximum interaction penetration score. We also conducted a perceptual study where participants are shown a side-by-side comparison of results from two methods and asked to choose the one perceptually more natural. We report the rate of being chosen as the better result.

The evaluation results are shown in Tab. 3. Our method generates high-quality results of human-scene interactions in cluttered environments. Our results achieve higher contact scores and less penetration with the scenes compared to SAMP. In addition, our method generates perceptually more natural results according to perceptual study.

5. Conclusion

In this paper, we leverage reinforcement learning to establish a framework to synthesize inhabiting behavior of virtual humans in indoor scenes, which is stochastic, realistic, and perpetual. The proposed method has large potential to improve many applications such as daily-living activity simulation, synthetic data creation, architecture design, and so on. Compared to existing methods, our method realizes fine-grained control by using body surface keypoints as targets, and achieves autonomous body-scene collision avoidance by incorporating scene perception into the states and the rewards. Experiments show that our method effectively enables virtual humans to inhabit the virtual, and outperforms baselines consistently. Our current study focuses on behavior synthesis in static scenes. We aim to extend our methods to scenes with dynamic objects in future work, in order to deliver a coherent system of simulating more complex human-scene interaction behaviors.

References

- [1] Kevin Bergamin, Simon Clavet, Daniel Holden, and James Richard Forbes. DReCon: data-driven responsive control of physics-based characters. *ACM Transactions On Graphics (TOG)*, 38(6):1–11, 2019. Publisher: ACM New York, NY, USA. 3
- [2] Michael Buttner. Machine learning for motion synthesis and character control in games. *Proc. of I3D 2019*, 2, 2019. 2
- [3] Michael Büttner and Simon Clavet. Motion matching-the road to next gen animation. *Proc. of Nucl. ai*, 2015(1):2, 2015. 2
- [4] Angel X Chang, Thomas Funkhouser, Leonidas Guibas, Pat Hanrahan, Qixing Huang, Zimo Li, Silvio Savarese, Manolis Savva, Shuran Song, and Hao Su. Shapenet: An information-rich 3d model repository. *arXiv preprint arXiv:1512.03012*, 2015. 6, 7
- [5] Helmut Grabner, Juergen Gall, and Luc Van Gool. What makes a chair a chair? pages 1529–1536. IEEE, 2011. 3
- [6] Abhinav Gupta, Scott Satkin, Alexei A Efros, and Martial Hebert. From 3d scene geometry to human workspace. pages 1961–1968. IEEE, 2011. 3
- [7] Ikhsanul Habibie, Daniel Holden, Jonathan Schwarz, Joe Yearsley, and Taku Komura. A recurrent variational autoencoder for human motion synthesis. 2017. 3
- [8] Peter E Hart, Nils J Nilsson, and Bertram Raphael. A formal basis for the heuristic determination of minimum cost paths. *IEEE transactions on Systems Science and Cybernetics*, 4(2):100–107, 1968. Publisher: IEEE. 2, 4
- [9] Mohamed Hassan, Duygu Ceylan, Ruben Villegas, Jun Saito, Jimei Yang, Yi Zhou, and Michael J Black. Stochastic scene-aware motion prediction. pages 11374–11384, 2021. 3, 4, 6, 7, 8
- [10] Mohamed Hassan, Vasileios Choutas, Dimitrios Tzionas, and Michael J Black. Resolving 3D human pose ambiguities with 3D scene constraints. pages 2282–2292, 2019. 4, 7
- [11] Mohamed Hassan, Partha Ghosh, Joachim Tesch, Dimitrios Tzionas, and Michael J Black. Populating 3D scenes by learning human-scene interaction. pages 14708–14718, 2021. 3, 6
- [12] Mohamed Hassan, Yunrong Guo, Tingwu Wang, Michael Black, Sanja Fidler, and Xue Bin Peng. Synthesizing Physical Character-Scene Interactions, Feb. 2023. arXiv:2302.00883 [cs]. 3
- [13] Daniel Holden, Oussama Kanoun, Maksym Perepichka, and Tiberiu Popa. Learned motion matching. *ACM Transactions on Graphics (TOG)*, 39(4):53–1, 2020. Publisher: ACM New York, NY, USA. 2
- [14] Daniel Holden, Taku Komura, and Jun Saito. Phase-functioned neural networks for character control. *ACM Transactions on Graphics (TOG)*, 36(4):1–13, 2017. Publisher: ACM New York, NY, USA. 3
- [15] Daniel Holden, Jun Saito, and Taku Komura. A deep learning framework for character motion synthesis and editing. *ACM Transactions on Graphics (TOG)*, 35(4):1–11, 2016. Publisher: ACM New York, NY, USA. 3
- [16] Ruizhen Hu, Zihao Yan, Jingwen Zhang, Oliver Van Kaick, Ariel Shamir, Hao Zhang, and Hui Huang. Predictive and generative neural networks for object functionality. *arXiv preprint arXiv:2006.15520*, 2020. 3
- [17] Kacper Kania, Marek Kowalski, and Tomasz Trzcinski. TrajeVAE: Controllable Human Motion Generation from Trajectories. *arXiv preprint arXiv:2104.00351*, 2021. 3
- [18] Lucas Kovar, Michael Gleicher, and Frédéric Pighin. Motion graphs. In *ACM SIGGRAPH 2008 classes*, pages 1–10. 2008. 2
- [19] Peizhuo Li, Kfir Aberman, Zihan Zhang, Rana Hanocka, and Olga Sorkine-Hornung. Ganimator: Neural motion synthesis from a single sequence. *ACM Transactions on Graphics (TOG)*, 41(4):1–12, 2022. Publisher: ACM New York, NY, USA. 3
- [20] Xueting Li, Sifei Liu, Kihwan Kim, Xiaolong Wang, Ming-Hsuan Yang, and Jan Kautz. Putting humans in a scene: Learning affordance in 3d indoor environments. pages 12368–12376, 2019. 3
- [21] Hung Yu Ling, Fabio Zinno, George Cheng, and Michiel Van De Panne. Character controllers using motion vaes. *ACM Transactions on Graphics (TOG)*, 39(4):40–1, 2020. Publisher: ACM New York, NY, USA. 2, 3
- [22] Libin Liu, KangKang Yin, and Baining Guo. Improving sampling-based motion control. volume 34, pages 415–423. Wiley Online Library, 2015. Issue: 2. 3
- [23] Libin Liu, KangKang Yin, Michiel Van de Panne, Tianjia Shao, and Weiwei Xu. Sampling-based contact-rich motion control. In *ACM SIGGRAPH 2010 papers*, pages 1–10. 2010. 3
- [24] Naureen Mahmood, Nima Ghorbani, Nikolaus F Troje, Gerard Pons-Moll, and Michael J Black. AMASS: Archive of motion capture as surface shapes. pages 5442–5451, 2019. 3, 4, 6
- [25] Josh Merel, Leonard Hasenclever, Alexandre Galashov, Arun Ahuja, Vu Pham, Greg Wayne, Yee Whye Teh, and Nicolas Heess. Neural probabilistic motor primitives for humanoid control. *arXiv preprint arXiv:1811.11711*, 2018. 3
- [26] Georgios Pavlakos, Vasileios Choutas, Nima Ghorbani, Timo Bolkart, Ahmed AA Osman, Dimitrios Tzionas, and Michael J Black. Expressive body capture: 3d hands, face, and body from a single image. pages 10975–10985, 2019. 2, 3
- [27] Xue Bin Peng, Pieter Abbeel, Sergey Levine, and Michiel Van de Panne. Deepmimic: Example-guided deep reinforcement learning of physics-based character skills. *ACM Transactions On Graphics (TOG)*, 37(4):1–14, 2018. Publisher: ACM New York, NY, USA. 3
- [28] Xue Bin Peng, Yunrong Guo, Lina Halper, Sergey Levine, and Sanja Fidler. Ase: Large-scale reusable adversarial skill embeddings for physically simulated characters. *ACM Transactions On Graphics (TOG)*, 41(4):1–17, 2022. Publisher: ACM New York, NY, USA. 2, 3
- [29] Xue Bin Peng, Angjoo Kanazawa, Jitendra Malik, Pieter Abbeel, and Sergey Levine. Sfv: Reinforcement learning of physical skills from videos. *ACM Transactions On Graphics (TOG)*, 37(6):1–14, 2018. Publisher: ACM New York, NY, USA. 3

- [30] Mathis Petrovich, Michael J Black, and Gül Varol. Action-conditioned 3D human motion synthesis with transformer VAE. pages 10985–10995, 2021. 3
- [31] Mathis Petrovich, Michael J Black, and Gül Varol. TEMOS: Generating diverse human motions from textual descriptions. pages 480–497. Springer, 2022. 3
- [32] Abhinanda R Punnakal, Arjun Chandrasekaran, Nikos Athanasiou, Alejandra Quiros-Ramirez, and Michael J Black. BABEL: bodies, action and behavior with English labels. pages 722–731, 2021. 6
- [33] Manolis Savva, Angel X Chang, Pat Hanrahan, Matthew Fisher, and Matthias Nießner. SceneGrok: Inferring action maps in 3D environments. *ACM transactions on graphics (TOG)*, 33(6):1–10, 2014. Publisher: ACM New York, NY, USA. 3
- [34] John Schulman, Filip Wolski, Prafulla Dhariwal, Alec Radford, and Oleg Klimov. Proximal policy optimization algorithms. *arXiv preprint arXiv:1707.06347*, 2017. 4, 5
- [35] Greg Snook. Simplified 3D movement and pathfinding using navigation meshes. *Game programming gems*, 1(1):288–304, 2000. Publisher: Charles River Media Newton Centre, MA, USA. 2, 4
- [36] Sebastian Starke, Ian Mason, and Taku Komura. Deepphase: Periodic autoencoders for learning motion phase manifolds. *ACM Transactions on Graphics (TOG)*, 41(4):1–13, 2022. Publisher: ACM New York, NY, USA. 2
- [37] Sebastian Starke, He Zhang, Taku Komura, and Jun Saito. Neural state machine for character-scene interactions. *ACM Trans. Graph.*, 38(6):209–1, 2019. 2, 3, 7
- [38] Sebastian Starke, Yiwei Zhao, Taku Komura, and Kazi Zaman. Local motion phases for learning multi-contact character movements. *ACM Transactions on Graphics (TOG)*, 39(4):54–1, 2020. Publisher: ACM New York, NY, USA. 2
- [39] Julian Straub, Thomas Whelan, Lingni Ma, Yufan Chen, Erik Wijmans, Simon Green, Jakob J. Engel, Raul Mur-Artal, Carl Ren, Shobhit Verma, Anton Clarkson, Mingfei Yan, Brian Budge, Yajie Yan, Xiaqing Pan, June Yon, Yuyang Zou, Kimberly Leon, Nigel Carter, Jesus Briales, Tyler Gillingham, Elias Mueggler, Luis Pesqueira, Manolis Savva, Dhruv Batra, Hauke M. Strasdat, Renzo De Nardi, Michael Goesele, Steven Lovegrove, and Richard Newcombe. The Replica Dataset: A Digital Replica of Indoor Spaces, June 2019. arXiv:1906.05797 [cs, eess]. 8
- [40] Richard S Sutton and Andrew G Barto. *Introduction to reinforcement learning*, volume 135. MIT press Cambridge, 1998. 2, 4, 5
- [41] Xiangjun Tang, He Wang, Bo Hu, Xu Gong, Ruifan Yi, Qilong Kou, and Xiaogang Jin. Real-time controllable motion transition for characters. *ACM Transactions on Graphics (TOG)*, 41(4):1–10, 2022. Publisher: ACM New York, NY, USA. 3
- [42] Guy Tevet, Brian Gordon, Amir Hertz, Amit H Bermano, and Daniel Cohen-Or. Motionclip: Exposing human motion generation to clip space. pages 358–374. Springer, 2022. 3
- [43] Guy Tevet, Sigal Raab, Brian Gordon, Yonatan Shafir, Daniel Cohen-Or, and Amit H Bermano. Human motion diffusion model. *arXiv preprint arXiv:2209.14916*, 2022. 3
- [44] Jonathan Tseng, Rodrigo Castellon, and C Karen Liu. EDGE: Editable Dance Generation From Music. *arXiv preprint arXiv:2211.10658*, 2022. 3
- [45] Jingbo Wang, Yu Rong, Jingyuan Liu, Sijie Yan, Dahua Lin, and Bo Dai. Towards diverse and natural scene-aware 3d human motion synthesis. pages 20460–20469, 2022. 3
- [46] Jiashun Wang, Huazhe Xu, Jingwei Xu, Sifei Liu, and Xiaolong Wang. Synthesizing long-term 3d human motion and interaction in 3d scenes. pages 9401–9411, 2021. 3
- [47] Zhiyong Wang, Jinxiang Chai, and Shihong Xia. Combining recurrent neural networks and adversarial training for human motion synthesis and control. *IEEE transactions on visualization and computer graphics*, 27(1):14–28, 2019. Publisher: IEEE. 3
- [48] Ye Yuan, Jiaming Song, Umar Iqbal, Arash Vahdat, and Jan Kautz. PhysDiff: Physics-Guided Human Motion Diffusion Model. *arXiv preprint arXiv:2212.02500*, 2022. 3
- [49] Siwei Zhang, Yan Zhang, Qianli Ma, Michael J Black, and Siyu Tang. PLACE: Proximity learning of articulation and contact in 3D environments. pages 642–651. IEEE, 2020. 3, 6
- [50] Xiaohan Zhang, Bharat Lal Bhatnagar, Sebastian Starke, Vladimir Guзов, and Gerard Pons-Moll. Couch: towards controllable human-chair interactions. pages 518–535. Springer, 2022. 3
- [51] Yan Zhang, Michael J Black, and Siyu Tang. We are more than our joints: Predicting how 3d bodies move. pages 3372–3382, 2021. 2, 3
- [52] Yan Zhang, Mohamed Hassan, Heiko Neumann, Michael J Black, and Siyu Tang. Generating 3d people in scenes without people. pages 6194–6204, 2020. 3
- [53] Yan Zhang and Siyu Tang. The wanderings of odysseus in 3D scenes. pages 20481–20491, 2022. 2, 3, 4, 5, 7
- [54] Kaifeng Zhao, Shaofei Wang, Yan Zhang, Thabo Beeler, and Siyu Tang. Compositional human-scene interaction synthesis with semantic control. pages 311–327. Springer, 2022. 2, 3, 4, 6, 7
- [55] Yang Zheng, Yanchao Yang, Kaichun Mo, Jiaman Li, Tao Yu, Yebin Liu, C Karen Liu, and Leonidas J Guibas. Gimo: Gaze-informed human motion prediction in context. pages 676–694. Springer, 2022. 3
- [56] Fabio Zinno. Ml tutorial day: From motion matching to motion synthesis, and all the hurdles in between. *Proc. of GDC 2019*, 2, 2019. 2